



Grao en Química

**Traballo Fin de
Grao**

*Polymer-assisted
deposition of
epitaxial oxide thin
films.*

Francisco Rivadulla Salgueiro

Xullo 2015

CURSO 2014-2015

Facultade de Química, University of Santiago de Compostela.

Autorization Sheet

Bachelor work (traballo de fin de grao) developed at CiQUS (Centro Singular de Investigación en Química Biolóxica e Materiais Moleculares, USC) and presented at Facultade de Química of the Universidade de Santiago de Compostela by **FRANCISCO RIVADULLA SALGUEIRO**, as a requisite to obtain the title of Grao en Química. This is presented after the authorization by Prof. **FRANCISCO RIVADULLA FERNÁNDEZ** and Ph.D. **BEATRIZ RIVAS MURIAS**, for its presentation and defense.

Signed:

Francisco Rivadulla Fernández

Beatriz Rivas Murias

Francisco Rivadulla Salgueiro

CONTENTS

1. SUMMARY	6
2. INTRODUCTION	7
2.1. The importance of thin films.	
2.2. Epitaxial growth and lattice mismatch.	
2.3. Synthesis of thin films.	
2.4. Polymer Assisted Deposition (PAD).	
2.5. Thin-films of metallic oxides.	
2.6. Perovskite structure.	
2.7. Oxides synthesized, some characteristics and properties.	
3. OBJECTIVES OF THIS WORK.	19
4. EXPERIMENTAL	20
4.1. Spin-coating process.	
4.2. Inductively Couple Plasma-Optical Emission Spectroscopy (ICP-OES).	
4.3. Thermogravimetric Analysis (TGA).	
4.4. Ultraviolet–visible Spectroscopy (UV-Vis).	
4.5. X-ray Diffraction techniques (XRD).	
4.6. Atomic Force Microscopy (AFM).	
4.7. Electrical transport measurements.	
4.8. Magnetic measurements.	
5. RESULTS AND DISCUSSION.	29
5.1. Thermogravimetric characterization of polymers.	
5.2. Preparation and deposition of the solutions.	
5.3. Synthesis of BiFeO ₃ (BFO) thin films.	
5.4. Synthesis of SrRuO ₃ (SRO) thin films.	
5.5. Synthesis of La _{0.7} Sr _{0.3} MnO ₃ (LSMO) thin films.	
5.6. Synthesis of a bilayer: BiFeO ₃ on La _{0.7} Sr _{0.3} MnO ₃ on SrTiO ₃ substrate (BFO/LSMO@STO).	
6. CONCLUSIONS	47

1. SUMMARY.

The possibility of growing epitaxial thin-films has been intensely studied during the last decades. The development of the physical deposition techniques, such as Pulsed Laser Deposition (PLD), Sputtering or Molecular Beam Epitaxy (MBE) made possible the production films and multilayers of very high quality, although they have the serious drawback of the huge price of the equipment, particularly for small-laboratory basic research.

For this reason, there is a great interest in developing more cost-effective chemical methods of deposition, which however must produce films of a quality similar to the physical techniques to meet the requirements of demanding applications.

In this work we use a chemical method to grow metal-oxide thin films of a structural and morphological quality which is similar to that obtained by traditional physical high-vacuum methods. The process basis is the preparation of solutions containing the metal-cations precursors of the thin film; a soluble metal salt, a complexing agent and a polymer for retaining the cations are the basic components of the precursor solutions used in this study. By spin-coating the solutions over commercial monocrystalline substrates (like (001) oriented SrTiO_3) and after a thermal treatment, thin-films of the materials of interest are obtained. A good control over the thickness and stoichiometry can be achieved through the control of the initial concentration of the solutions and the gaseous atmosphere during the annealing.

In this study we obtained thin films epitaxially grown of BiFeO_3 , SrRuO_3 , $\text{La}_{0.7}\text{Sr}_{0.3}\text{MnO}_3$ and a bilayer of $\text{BiFeO}_3/\text{La}_{0.7}\text{Sr}_{0.3}\text{MnO}_3$.

These compositions were selected due to their scientific and technologic relevance. The structure and morphological characterization was carried out by X-ray and microscopy techniques. The electric and magnetic properties are also investigated to study the effect of the low dimensionality and epitaxial strain in these materials.

2. INTRODUCTION.

2.1. The importance of the thin films.

Nowadays, the development of synthesis method of high quality thin films is desirable due to its interesting applications in many areas of technology and in basic research. In this context, thin films are widely used in light emitting, in electronic devices of high temperature and high power, in microwave devices and micro-electromechanical, optical filters, photodiodes and sensors, cold cathodes, transparent transistors, photodetectors emitting diodes light and laser, magnetic storage memory; piezoelectric, ferroelectric devices and thermoelectric superconductors, etc.

Apart from these widespread uses, thin films are important owing to the possibility of the appearance of new phenomena and improved properties induced by the strain substrate. This strategy is called strain engineering. For example, strained thin films of LaCoO_3 shows a ferromagnetic-insulator behavior, with a $T_C \sim 85\text{-}90\text{ K}$ ^{1,2} although this material shows a diamagnetic response in bulk.

Other interesting example is the verification of the theoretical prediction that strain can induced a polar phase in SrMnO_3 compound,³ as it was demonstrated in SrTiO_3 grown on $\text{Si}(111)$.⁴

¹ D. Fuchs, E. Arac, C. Pinta, S. Schuppler, R. Schneider, H. v. Löhneysen, *Phys. Rev. B* **75**, 014434 (2008).

² F. Rivadulla, Z. Bi, E. Bauer, B. Rivas-Murias, J.M. Vila-Fungueiriño, Q. X. Jia, *Chem. Mater.* **25**, 55 (2013).

³ C. Becher, L. Maurel, U. Aschauer, M. Lilienblum, C. Magén, D. Meier, E. Langenberg, M. Trassin, J. Blasco, I. P. Krug, P. A. Algarabel, N. A. Spaldin, J. A. Pardo & M. Fiebig, *Nature Nanotechnol.*, doi:10.1038/nnano.2015.108.

⁴ J.C. Woicik, E.L. Shirley, D.A. Fischer, S. Sambasivan, C.R. Ashman, C.S. Hellberg, P. Zschack, E. Karapetrova, P. Ryan, and H. Li, SRMS-5 Conference, Chicago July 30 – Aug 2 (2006).

2.2. Epitaxial growth and mismatch.

That is epitaxial growth means that a material must maintain a consistent crystallographic orientation and commensurability to the substrate on which it is grown.

When the composition of the film is different from the substrate, it is called heteroepitaxial growth. Homoepitaxial growth refers to equal composition materials in the film and substrate.

It is possible to calculate the epitaxial stress caused on a material growth in a given substrate by the f parameter (lattice mismatch). This can be calculated from the lattice parameters of the substrate and film:

$$f = \frac{a_{film} - a_{substrate}}{a_{substrate}}$$

If the in-plane a, b cell parameters of the film undergo a compression (expansion) the out of plane c lattice parameter undergoes a corresponding expansion (compression), so the volume is maintained (elastic deformation, in the absence of stoichiometry variations).⁵

There are three types of growth by the value of parameter f :

- **Growth in tensile stress or elongation (parameter values in the plane are lower than in the substrate).** The film undergoes a compression parameter c out of the plane with a value to $f < 0$.
- **Compressive stress growth (parameter values in the plane are higher than in the substrate).** The film shows or undergoes an elongation in its parameter out of plane (c) with a value to $f > 0$.
- **Relaxed growth.** Too large a difference between the values of the film and substrate in-plane lattice parameters. This large difference causes the nearest layer to the substrate being affected by growth stress. As the film grows thicker, the layers are no longer affected by stress. The material fails to manifest characteristic properties due to tension and behaves like bulk material.

⁵ M. Opel, *J. Phys. D: Appl. Phys* **45**, 033001 (2012).

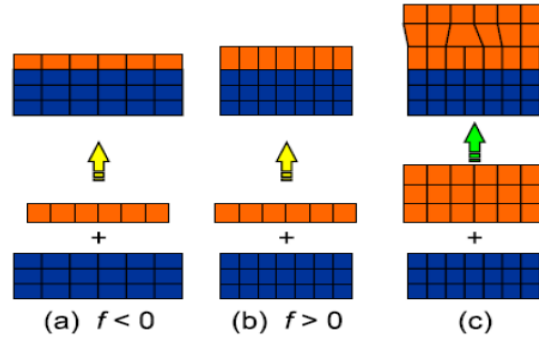


Figure 1. Scheme of the three modes of thin-film epitaxial growth, depending on the lattice mismatch with the substrate. a) $a_{\text{film}} < a_{\text{substrate}}$; b) $a_{\text{film}} > a_{\text{substrate}}$; c) $a_{\text{film}} \gg a_{\text{substrate}}$.

There are numerous commercially available substrates for deposition of thin films in a wide range of lattice parameters.

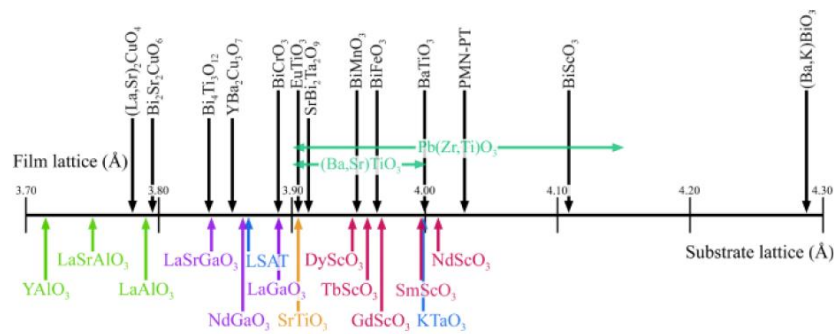


Figure 2. Commercial monocrystalline substrates with perovskite structure (pseudo-cubic or pseudo-tetragonal cells).

2.3. Synthesis of thin films.

The synthesis methods of thin films can be classified into two main groups: physical and chemical techniques.

- **Physical techniques.** The most used are molecular beam epitaxy (MBE), and Physical Vapour Deposition (PVD); where stand out Pulsed Laser Deposition (PLD), Electron Beam Physical Vapour Deposition (EBPVD); and sputtering deposition. All of them share the transfer of precursors to a substrate and their nucleation under high vacuum.

- **Chemical techniques.** This type of techniques includes Metal Organic Vapour Deposition (MOVD) or Sol-Gel Deposition among others. The most suitable techniques for scalability are those starting from a solution, as they do not require large high-vacuum equipment.

During the last decade, chemical deposition techniques have played an exceptionally important role in the design and manufacture of novel advanced devices. Physical deposition techniques has the advantages of well controlled film thickness, high purity, and desired physical properties, but suffer from limitations such as high cost of necessary equipment, the restriction of coatings on a relatively small area, poor conformality, low throughput, restricted directional variation, and reduced compositional control.

Thin films of metallic oxides are essential parts of semiconductors. These types of films can also have benefits as coatings that are resistant to a number of environmental effects. Unfortunately, growing metal-oxide films requires large, expensive equipment. Capital costs for a single metal-oxide films deposition machine can run from \$500,000 to \$3.5 million, and only very small films can be grown using traditional methods.⁶

Some of these issues can be addressed using chemical deposition techniques, although the reproducibility and quality of the films in the ultra-low thickness range (less than 20 nm) is still not competitive with physical methods.

Chemical-solution depositions such as sol-gel are more cost-effective, but many metal oxides cannot be deposited and the control of stoichiometry is not always possible owing to differences in chemical reactivity among the metals.^{7,8} Moreover, the large surface roughness makes impossible sequential deposition of heteroepitaxial multilayers.

In 2004 Jia et al.⁹ have reported an interesting and novel chemical process to grow high quality metal-oxide films, so-called Polymer Assisted Deposition (PAD). This method is simple, low-cost and based on aqueous solutions of polymers. This method also overcomes the important limitation of other techniques related to the coating over large

⁶ <http://techportal.eere.energy.gov/technology.do/techID=217#contactForm>

⁷ S. M. Pawar, B. Pawar, J. H. Kim, S. Joo and C. Lokhande, *Curr. Appl. Phys.* **11**, 117 (2011).

⁸ G. F. Zou, J. Zhao, H. M. Luo, T. M. McCleskey, A. K. Burrell, Q. X. Jia, *Chem. Soc. Rev.* **42**, 439 - 449 (2013).

⁹ Q. X. Jia, T. M. McCleskey, A. K. Burrell, Y. Lin, G. E. Collis, H. Wang, A. D. Q. Li & S. R. Foltyn, *Nat. Mater.* **3**, 529-532 (2004).

areas, reaching continuous thin films up to cm² scale.¹⁰ Through this technique it was possible to synthesize a wide variety of oxide films and others films including many non-oxide materials such as nitrides (TiN, AlN or GdN) and carbides (NbC).¹¹

2.4. Polymer Assisted Deposition (PAD).

The polymer assisted deposition (PAD) method is based on the complexation of metal cations with a polymer, which also controls the viscosity of the solution to obtain high quality thin-films after spin coating in a substrate and thermal annealing.¹⁰

We show in this project that PAD can be used to grow high-quality thin films of transition metal-oxides, in a wide range of compositions and over cm areas. The quality of the films; the control of stoichiometry and cristallinity is comparable to physical methods in the ultrathin limit. Rather than spray a precise amount of material in a high vacuum, which requires the expensive equipment like PLD (pulse-laser deposition), we solubilize the metal oxides in inexpensive polymers, then bake off the polymer, leaving a uniform thin film of metal oxide deposited on the substrate. PAD is also superior to sol-gel methods because PAD can be used with many more metal oxides; the thin film is uniform and not susceptible to cracking; and because the metal-oxide stoichiometry can be precisely controlled.

The principal polymer used for the preparation of the solutions is the polyethyleneimine (PEI), a water soluble biocompatible polymer which eliminates the need of organic solvents in the process. We have observed no differences in the performance of linear or branched PEI, therefore being not sensitive to different commercially available PEI.

¹⁰ J.M. Vila-Funqueiriño, B. Rivas-Murias, B. Rodríguez-González, O. Txoperena, D. Ciudad, L. E. Hueso, M. Lazzari, and F. Rivadulla, *ACS Appl. Mater. Interfaces* **7**, 5410-5414 (2015).

¹¹ G. Zou, H. Luo, Y. Y. Zhang, J. Xiong, Q. M. Wei, M. J. Zhuo, J. Y. Zhai, H. Y. Wang, D. Williams, N. Li, E. Bauer, X. H. Zhang, T. M. McCleskey, Y. R. Li, A. K. Burrell, Q. X. Jia, *Chem. Commun.* **46**, 7837-7839 (2010).

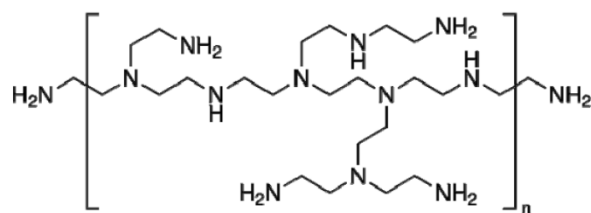


Figure 3. PEI structure.

Linear PEI has only secondary amino groups, unlike the branched PEI, containing the three types of amino groups (primary, secondary and tertiary).¹² The metal cations are complexed with ethylenediaminetetraacetic acid (EDTA). The pH is then controlled so that negatively charged complexes, $[\text{EDTA-M}^{n+}]^{(4-n)-}$ are easily retained by the cationic PEI chains via a combination of hydrogen bonding and electrostatic interactions.⁹

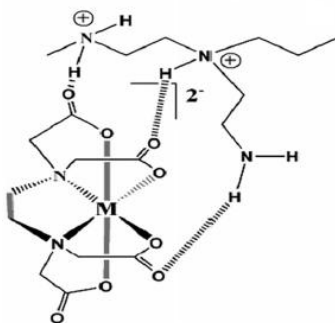


Figure 4. Schematic illustration of the interaction among the coordination complexes of EDTA-metal and PEI.¹

So far, good complexation of PEI was observed with metals of the first transition row and alkaline-earths, obtaining stable solutions over time.¹³

PEI decomposes thermally above 575°C, without leaving any carbon residue, and therefore a post-treatment cleaning synthesis is not necessary.

PAD process consists of several steps, which include preparation of solution and growth of the film.

¹² A. von Harpe, H. Petersen, Y. Li, *J. Control. Release* **69**, 309-322 (2000).

¹³ A. K. Burrell, T. M. McCleskey, Q. X. Jia, *Chem. Commun.* **11**, 1271- 1277 (2008).

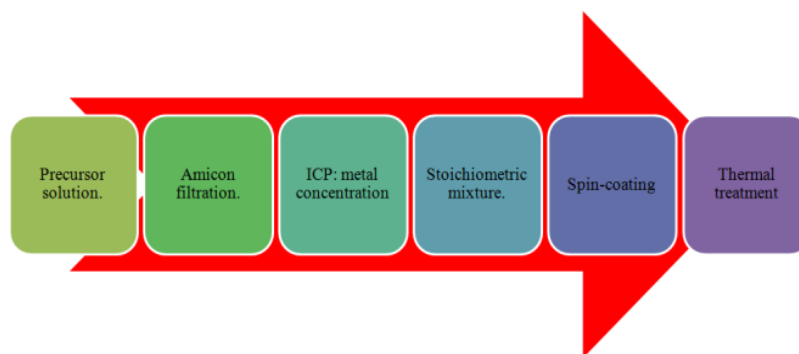


Figure 5. Different steps of the process of PAD synthesis of thin-films.

Preparation of precursor solutions

The first step of PAD process is obtaining stable solutions of the metals that will form the mixed oxide of interest. The usual procedure is to dissolve metal salts such as chlorides, nitrates or acetates, in a solution of EDTA and PEI in water. In this step, the pH is an important factor to control, because it controls the metal hydrolysis (giving oxides or hydroxides), and metal complexation with EDTA, therefore being the ultimate factor of control of the interactions of metal cations with PEI. pH adjustment can be carried out by addition of acidic (HCl) or basic (NH₄OH) solutions and varying the EDTA-PEI relationship because each compound is different in nature (EDTA is acidic and PEI is basic PEI).

Purification of the solutions

After preparation of the polymeric solutions, we performed a filtration under pressure with AMICON *Stirred Ultrafiltration Cell* (Millipore) with 10 kDa filters. This removes the anions of the precursor salts, traces of PEI of low molecular weight EDTA-Metal complex poorly coordinated to PEI, and not coordinated metal cations. Very importantly, we have identified small polymeric fractions (≈ 5 kDa) of highly branched structures, which present very different physical and chemical properties (particularly a much smaller solubility) to larger and less branched PEI molecules. These are present in all commercial PEI, due to the synthetic method used to prepare these polymers, and therefore it is imperative to remove them before spin-coating deposition, in order to avoid the formation of defects in the final film.⁹

Cation concentration analysis (ICP-OES).

After the filtration the solutions were analyzed by optical emission spectroscopy-inductively coupled plasma (ICP-OES) in order to determine the concentration of metals in solutions. This is important to establish a stoichiometric ratio required for proper growth of the film. Once we know the exact concentration of cations in solution, we can concentrate or dilute them to obtain a concentration required for the deposition and to control the viscosity of the final mixture to the spin-coating process.

Spin-coating.

The obtained mixture solution is deposited by spin-coating on substrates of SrTiO₃ (001). This process depends on factors such as concentration and solution viscosity, and varying parameters in the spin-coating equipment. Controlling the acceleration and deceleration ramp or the maximum rotation speed, we can control the thickness of the films.

It is vital the cleaning of the substrates, because for uniformity and homogeneity in the films, the solution must be able to expand without any hurdle on the substrate surface. For example, silica substrates require a process of hydrophilization for aqueous solutions to be retained on the substrate, and not be expelled from the surface by centrifugal force.¹⁴

Thermal treatment.

In the final step, the polymer film is subjected to heat treatment in an oven. Decomposition requirements are determined by the final composition of the film and involve different parameters: temperature ramp rate, final temperature, atmosphere, (for example, sometimes it is necessary a reducing or oxidant atmosphere) etc; factors that decompose and eliminate the polymer without leaving any residue and therefore forming crack-free films.

¹⁴ V. E. Agabekov, G. K Zhavnerko, *Russ. J. Gen. Chem.* **77**, 343-349 (2007).

2.5. Thin films of metallic oxides.

Metal-oxides are emerging as important materials for their versatile properties such as high-temperature superconductivity, ferroelectricity, ferromagnetism, piezoelectricity and semiconductivity. These properties make them very attractive for application in electronic and optical devices.

The main challenge in fabricating such devices is in producing high-quality, well-oriented films with minimal structural and chemical imperfections.

Metal oxides have been the subject of efforts in the field of research, since these materials are linked to some of the most important advances in the physical chemistry of the solid state physics.

In most high-performance devices, epitaxial films are desired because of their sensitivity to strain of their electronic and magnetic properties. In other words, the properties and functionality of films can easily be tuned through strain engineering.

2.6. Perovskite structure.

Oxide-perovskites are compounds with stoichiometry ABO_3 , receiving its name from an oxide of Ca and Ti with cubic structure, $CaTiO_3$. Atoms A and B are metal cations and one of the distinguishing features of the perovskites over other families of oxides is the wide range of substitutions that can accept its crystallographic structure (about 25 elements that can occupy position A and almost 50 different elements capable of occupying site B). The cation A is the largest atomic radius is the center of the cube, the cation B occupies the eight vertices of the cube and the center of the edges of the cell are centered oxygen atoms. Each cation B, which defines the vertex of neighboring cubes, is strongly bonded to the six oxygen atoms surrounding it, belonging to each of the six cube edges converging at the apex. Oxygen defines the vertices of an octahedron. The cation A, previously seen as the center of a cube, is now seen

surrounded by eight octahedron with shared vertices, each of which contains a cation B in the center.¹⁵

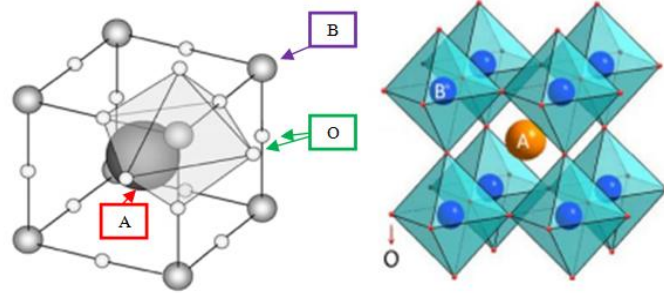


Figure 6. Perovskite structure of mixed oxide and arrangement of the 8 octahedrons around the atom A.¹⁶

Generally, all mixed oxides with perovskite structure lose their cubic arrangement below a critical temperature (T_c), due to structural transitions that reduce their symmetry. These deviations from the cubic cell give rise to many types of compounds, we can quantify the distortion by “Goldschmidt tolerance factor”¹⁷, that predicts the symmetry of the structures based on the size of the ionic radii of the elements that it composes:

$$t = \frac{r_A + r_O}{\sqrt{2}(r_B + r_O)}$$

where t is “Goldschmidt tolerance factor”, and the r_A , r_B and r_O are the ionic radii to cations **A**, **B** and oxygen atoms respectively. Thus, a value of t equal to unity is consistent with a cubic structural arrangement. Compression of the B-O bonds and elongation of the A-O bonds reduces t and gives place to structures such as tetragonal, orthorhombic or monoclinic. Conversely, compression of A-O and elongation of B-O stabilize the hexagonal symmetry.

These distortions are accommodated by cooperative rotations of the octahedrons around a particular crystallographic axis, improving packaging and therefore decreasing the energy of the crystal.¹⁸

¹⁵ A. M. Glazer *Acta Crystallogr. B* **28**, 3384 (1972); A. M. Glazer. *Acta Crystallogr. A* **31**, 756 (1975).

¹⁶ <http://www.bdigital.unal.edu.co/4261/2/2299928.20112.pdf>

¹⁷ V. M. Goldschmidt, “Geochemische Verteilungsgesetze der Elemente VII-VIII” *Skrifter Norske Videnskaps Akademi*, Oslo (1926).

¹⁸ P. Kayser González, “Nuevas perovskitas dobles obtenidas en condiciones extremas de presión y temperatura”, Universidad Complutense de Madrid (2014).

2.7. Oxides synthesized, some characteristics and properties.

BiFeO₃

In multiferroic materials, magnetism and ferroelectricity coexist, and if they are coupled they give rise to magnetoelectricity (or ferroelectromagnetism). Since most ferromagnets are conductive and ferroelectrics are insulating, ferromagnetic ferroelectrics are scarce, particularly at or above room temperature. BiFeO₃ (BFO) is one of the most studied multiferroic materials.

At room temperature, bulk BFO exhibits a rhombohedrally distorted perovskite structure, with pseudocubic lattice parameters $a_r = 3.965 \text{ \AA}$ and $\alpha_r = 89.4^\circ$. BFO has an incommensurate G-type antiferromagnetic (AFM) structure ($T_N = 650 \text{ K}$) and ferroelectricity ($T_C = 1103 \text{ K}$) caused by $6s^2$ lone pair distortions of Bi³⁺ at the A-site. BFO is a material at room temperature with small energy band gap (2.5 eV) and a very large remnant ferroelectric polarization ($\sim 100 \mu\text{C}/\text{cm}^2$).^{19,20}

SrRuO₃

Ferromagnetic conductive oxide SrRuO₃ (SRO), which has a Curie temperature of around 160 K, has been widely studied recently for electronic device applications because of its high electrical conductivity, crystal structure compatibility with many other technically important metal oxides, and high thermal and chemical stability. For example, epitaxial thin films of SRO have been used as bottom electrodes for ferroelectric capacitors, buffer layers for coated conductors, normal metal layers for superconductor Josephson junctions, and ferromagnetic metal layers in spin-polarized ferromagnetic tunnel junctions.²¹ Bulk SRO crystallizes in an orthorhombic structure with lattice parameters $a = 5.5670 \text{ \AA}$, $b = 5.5304 \text{ \AA}$, and $c = 7.8446 \text{ \AA}$; its lattice parameter is 3.930 \AA in pseudocubic notation.²²

¹⁹ G. A. Smolenskii, I. Chupis, *Sov. Phys. Usp.* **25**, 475 (1982).

²⁰ F. Kubel, H. Schmid, *Acta Crystallogr. B* **46**, 698 (1990).

²¹ C. B. Eom, R. J. Cava, R. H. Fleming, J. M. Phillips, R. B. van Dover, J. H. Marshall, J. W. P. Hsu, J. J. Krajewski, W. F. Peck, *Jr. Science* 258:1766 (1992).

²² X. W. Wang, X. Wang, Y. Q. Zhang, Y. L. Zhu, Z. J. Wang et al., *J. Appl. Phys.* **107**, 113925 (2010).

Reduced Curie temperatures have been observed for thin films of SrRuO₃ deposited on substrates with mismatched lattice parameters and explained in terms of strain effects.²³

La_{0.7}Sr_{0.3}MnO₃

Doped perovskite manganites have renewed interest because they exhibit a variety of unique magnetic, electronic and transport behaviors. Half-metallic ferromagnetic materials appear as potential candidates for spintronic devices, and much work is under progress to synthesize magnetic oxides, such as La_{0.67}Sr_{0.33}MnO₃ (LSMO).

LSMO undergoes an anti-ferromagnetic and insulating behavior at high and low doping concentration (x) values. The system becomes ferromagnetic and metallic in a certain range of concentrations centered around $x \approx 0.33$ with highest Curie temperature ($T_c = 370\text{K}$). So it is considered for the use in various devices such as magnetic field sensors and hard disk read heads. Moreover, due to the hole doping in LSMO, many interesting device applications have been proposed based on LSMO. LSMO is rhombohedral, in the pseudocubic description, the unit cell angle α and the lattice parameter of LSMO are 90.26° and 3.88 \AA , respectively.

The magnetic and transport properties of manganite thin films are very sensitive to its micro structure, growth conditions, and the lattice strain induced by the underlying substrate.²⁴

²³ J. J. Neumeier, A. L. Cornelius and J. S. Schilling, *Physica B* **198**, 324 (1994).

²⁴ M. C. Martin and G. Shirane, *Phys. Rev B* **53**, 14285- 14290 (1996).

3. OBJECTIVES OF THIS WORK.

The main objective of this project is to obtain thin films of nanometric thickness by a chemical deposition method, with the same quality as those obtained through physical deposition methods (Pulsed Laser Deposition or Molecular Beam Epitaxy).

Chemical technique used in this project to obtain thin films is called the Polymer Assisted Deposition (PAD), a method based on the use of aqueous solutions of metal cations whose preparation involves a much lower cost than any equipment used in a physical technique.

To obtain thin films of high quality must ensure certain important parameters: epitaxial growth, namely, growth of samples with the same orientation and structural relationship to the substrate on which is deposited; homogeneity and low surface roughness for films; coating large areas (cm^2); and controlling the thickness and stoichiometry of the films.

The physical properties (magnetic and electronic transport) will be used to test the validity of the films.

4. EXPERIMENTAL.

4.1. Spin-coating process.

Spin-coating has been used for decades for fabrication of thin films. The process itself consists of depositing a small amount of solution onto the center of a substrate, rotating at high speed.²⁵ In our case we used a model spin-coater WS-650-23 NPP Laurell. The technique is widely used and it is based mainly on centrifugal force achieved due to the high rotational speed of the substrate, fixed to the base of the spin coater by vacuum. This causes the spreading of the solution throughout the substrate surface, reaching a homogeneous solution layer covering the entire substrate.

The quality of the spin-coated films depends on several factors:

- **Solution:** volume, viscosity, concentration and surface tension.
- **Substrate:** roughness, hydrophobic effects and superficial dimension.
- **Other conditions:** rotational speed, acceleration, dwell time, temperature and environmental humidity.

The volume of solution used for depositions in our study ranges between 20 and 40 μL with a metal concentration of 120 - 300 mM. The environmental conditions were 17 - 25 °C of temperature and 50 - 70 % of humidity. The substrates were 5 x 5 mm of size and a rotational speed of 2000 - 4500 rpm.

4.2. Inductively Couple Plasma-Optical Emission Spectroscopy (ICP-OES).

This technique is used to determine the metal concentration from solutions used in thin film deposition. In inductively coupled plasma optical emission spectrometry (ICP-

²⁵ Massey et al. US 4267212 A “Glass Slurry Deposition”, *IBM Technical Disclosure Bulletin* **14**, 10 (1972).

OES), the samples are transported into the plasma by a current flow of liquid through a quartz tube becoming an aerosol upon arrival at the nebulizer, where the liquid is separated into scattered drops and enters the plasma. Once in the plasma, the sample undergoes several consecutive processes: desolvation, vaporization, atomization and excitation or ionization. Atoms or ions introduced in the plasma emit a characteristic wavelength, which becomes useful information about concentration.²⁶

There are several intense lines which can identify and quantify the most atoms of the periodic table elements (over 70 elements); however, it depends on the selection matrix or concentration in which our analyte are (detection limits). Samples must be properly filtered solutions, and the volume required will depend on the number of items to be measured, generally require 10 to 15 mL of filtered solution.²⁷

The model of own ICP-OES spectrometer is *PerkinElmer AS93-plus* (general service of USC, CACTUS Lugo).

4.3. Thermogravimetric Analysis (TGA).

Thermogravimetric analysis (TGA) in inert atmosphere is used as a method for empirically assessing the thermal stability of PEI. Equipment used for our analysis, *TA Instruments Q5000*(general equipment of CIQUS), allows to analyze our polymers in the same conditions which they are subjected to during the heat treatment in the furnace (muffle or tube) in air or oxygen atmosphere; with temperature ranges and heating ramps also similar to those used in that process. When working with polymers, is advisable to work with the same amounts in the times of performing the analysis to avoid drifts in the data (similarly by using a heating ramp).

²⁶ Douglas A. Skoog, F. James Holler, Stanley R. Crouch. 2008. “*Principios de Análisis Instrumental*”. 6ª Ed. México: Cengage Learning. ISBN-10: 970-686-829-1.

²⁷ <http://www.usc.es/gl/investigacion/riaidt/analise/icpo.html>

4.4. Ultraviolet–visible Spectroscopy.

Molecular absorption spectroscopy is based on measuring the transmittance (T) or the absorbance (A) of solutions found in transparent cells with length b . In the moderate-low concentration range, the concentration of the analyte is linearly related to the value of the absorbance, according to the Beer's law:

$$A = -\log T = \log \frac{I_0}{I} = \epsilon cb$$

Where A is the absorbance, T transmittance, I_0 and I is the radiant incident and transmitted intensities, respectively, ϵ is the analyte's molar absorptivity, b pathlength cell and c is the concentration of the analyte to be measured.

At higher concentrations the degree of interactions between solvent-solute and solute-solute is too high and may affect the absorption of the analyte; the closeness of ions in solution and other species also distorting the absorptive capacity of the analyte.²⁶

This technique provided us with information about the concentrations of ruthenium in the different solutions, and also allowed us to study the complexation equilibria Ru-EDTA through the variation in the complex transition band.

In this research, we have used a *Cary series, 300 UV-Vis Spectrophotometer (Agilent Technologies)*.

4.5. X-ray Diffraction techniques (XRD).

The X-ray diffraction is one of the physical phenomena that occur when interacting X-ray beam of a particular wavelength, with a crystalline substance. The X-ray diffraction is based on coherent scattering of X-ray beam by the sample (the wavelength of the radiation is maintained) and constructive interference of the waves are in phase and which are dispersed in certain directions of space. The phenomenon of diffraction can

be described by Bragg's Law, which predicts the direction in which constructive interference occurs between beams of X-rays scattered coherently by crystal:

$$n\lambda = 2d_{hkl}\sin\theta$$

where d_{hkl} is the distance between planes (it is the order of the X-ray's wavelength).

The equipment used was a *PANalytical Empyrean* with beam incident wavelength of 1.540598 Å (general services of USC). Its basic components are: an emission source of X-rays copper anode, a mobile platform and a detector sample. Platform allows the correction of the inclination by optimizing the position of the sample, also looking reflections of interest. We can do various actions with that equipment:

- ω . Angle of incidence of X-rays with the sample surface.
- 2θ . Angle between the X-ray and detector.
- ψ . Tilting of the sample.
- ϕ . Sample rotation in the plane.
- x,y . Sample displacement in the plane.
- z . Vertical displacement of the sample.

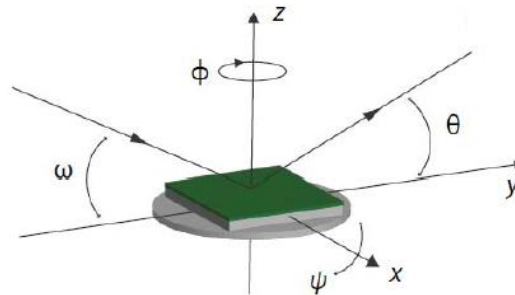


Figure 7. Principal equipment geometry angles to measurements.

Our study was conducted with different configurations of the X-ray source, the sample or the detector to obtain different information about our films:

- **$\theta - 2\theta$ measurements.** Such measurements give information about the orientation and cell parameters out of the plane of the film. In our case the substrates are in an orientation (001) and if samples grow oriented with respect

to the substrate STO (001), only the reflections in planes (001) should be observable. The cell parameter of the samples can be obtained according to:

$$d_{hkl} = \frac{a}{\sqrt{h^2+k^2+l^2}} \qquad a = \frac{\lambda\sqrt{h^2+k^2+l^2}}{2\sin\theta}$$

where a is the corresponding cell parameter and h , k and l are the Miller's indices of the plane. To make adjustments to the calculation of these parameters we were used the program *HighScore Plus*.

- **X-ray Reflectometry (XRR).** It is a technique that uses X-ray radiation to measure the reflected intensity at low angles. It is $\omega=2\theta$ scans, maintaining a constant ratio of $\omega=\theta$. As the signal obtained corresponds to the interference of the reflected radiation between layers of different density, determines the film thickness. For angles of incidence (θ) below the critical angle, penetration is very low and total external reflection occurs. Above this critical angle increases penetration and, due to interference between the x-ray beams constructively and destructively dispersed, oscillations that provide information about the film thickness are detected (the period of oscillations is inversely proportional to film thickness). The decay in signal intensity indicates the roughness, so that the greater the roughness of our film, the higher will be the intensity decay with the angle. The thickness can be obtained by making an adjustment with Fourier's Transform with *X'Pert Reflectivity* program, which uses the equation:

$$\theta_m^2 = \theta_c^2 + \left(\frac{\lambda}{2e}\right)^2 m^2$$

where θ_m is the maximum position, θ_c is the critical position, m is the order of the peak, e is the film's thickness and λ is the wavelength of X-rays. Thickness values can be obtained plotting $\theta_m^2 - m^2$ and taking the slope of the linear fit (p):

$$e = \frac{\lambda}{2\sqrt{p}}$$

- **Reciprocal Space Mapping (RSM).** It allows obtaining images in two dimensions around a reflection. When performed on a ($\omega=2\theta$) symmetrical reflection, we only get information about cell parameter out of the plane of the film; but if we do it around an asymmetric reflection, also provides information

about the cell parameters in the plane, giving valuable information to get a stress analysis between the substrate and the film. For the RSM it is necessary to make a series of sweeps in 2θ for a range of values to ω with ψ and φ constants, that is, the position of the detector is varied to different angles of incidence of the X-ray.

Coordinates in reciprocal space are Q_x (parallel to surface) and Q_z (perpendicular to the surface), and are described by the equations

$$Q_x = \sin \theta \sin(\theta - \omega)$$

$$Q_z = \sin \theta \cos(\theta - \omega)$$

defining the parameters in and out of the plane as:

$$a = \frac{\lambda \sqrt{h^2 + k^2}}{2Q_x}$$

$$c = \frac{\lambda l}{2Q_z}$$

where h , k and l are Miller's indices of the corresponding planes in the pseudocubic system and λ it is the wavelength of incident X-ray radiation.

4.6. Atomic Force Microscopy (AFM).

AFM is a kind of technique within the Scanning Probe Microscopy (SPM). AFM microscopy probes the surface of a sample with a tip very sharp, a few microns in length and less than 100 Å in diameter. The tip is located at the end of the cantilever of 100 to 200 microns long and the force (the most common being the van der Waals forces) between the tip and the sample surface causes the cantilever to bend or flex. These deflections are transmitted to a photodiode (detector) via a laser (on the top of the cantilever) and a topographic map of the surface is obtained. This type of measurement can be applied to any material, independently of their electrical conductivity.

The applications are varied: measurements of properties such as the surface conductivity, static load distribution, localized friction, magnetic fields, and elastic modulus.

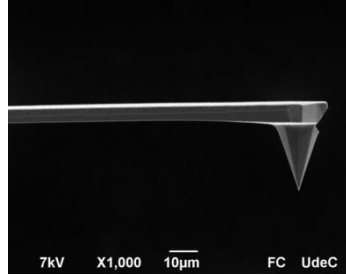


Figure 8. Image of a cantilever used in AFM.

In an AFM three basic modes of operation are distinguished: contact mode, non-contact mode and tapping mode, depending on the nature of the tip motion. The equipment used in this project was the *Park NX-10* in non-contact mode (general equipment of CIQUS).

4.7. Electrical transport measurements.

In order to eliminate the impedance contribution of the wires and contact resistance, electrical resistivity measurements were performed by using a "four contact configuration". In this configuration, the current I is driven into the sample through two wires and the voltage drop $\Delta V = V_1 - V_2$ is measured between two separated points of the sample. Knowing the values of I and ΔV the resistivity (ρ) is calculated by

$$\rho = R \frac{A}{d} = \frac{\Delta V}{I} \frac{t\omega}{d}$$

where R is the resistance calculated from Ohm's law $V = IR$, d is the distance between voltage contacts, and A is the cross-sectional area defined as the product of the thickness t and the width ω of the sample. Aluminium wire of 10 μm diameter is used for the contacts.

The current was injected by a dc Keithley source and the voltage drop was measured with a nanovoltmeter, also from Keithley.²⁸

Before measuring the electrical transport properties of the film they were lithographed by Ar plasma with a mask of molybdenum. To ensure good contact between the aluminium wire and the sample Cr/Au (5nm / 25nm) contacts were deposited by sputtering process.

Other electrical measurements were carried out in the Van der Pauw (VdP), configuration. In this case, the four ohmic contacts are placed in the corners of the sample, and the contacts should be as small as possible and the error because these will be a function of its diameter. Also the four contacts must be of the same material. This configuration avoids errors due to irregular sample shape and provides a more accurate absolute value of the resistivity.

Resistivity measurement was conducted using homemade equipment.

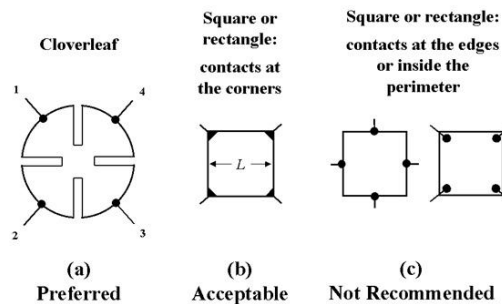


Figure 9. Possible arrangements for VdP measurements.

4.8. Magnetic measurements.

For magnetic measurements was used a Superconducting Quantum Interference Device (SQUID) *MPMS Evercool* from *Quantum Design*.

Aparallel or perpendicular magnetic field is applied to the sample at a certain temperature. The temperature range oscillates between 1.9 and 400 K and the DC applied field ranging is -7 – 7 Tesla.

²⁸ C. X. González Quintela, “Thermoelectric Properties of Chromium Nitride”, Universidade de Santiago de Compostela (2013).

The sample is positioned inside the superconducting ring, so it is under an even DC magnetic field applied on the film's plane; with everything cooled by helium. The sample is then displaced through the superconductive ring, inducing a current in the coils, proportional to the magnetic flux, which is detected by the SQUID, converting it into a voltage. Consequently the induced magnetic moment by the sample is proportional to voltage variation, with a resolution in the order of 10^{-6} emu (10^{-9} A.m²).

5. RESULTS AND DISCUSSION.

5.1. Thermogravimetric characterization of polymers.

In PAD process, an important step is to know the decomposition temperature of the used polymer for the depositions in order to totally remove it in the subsequent thermal treatment.

TGA is based on the mass loss of the polymer as the temperature increases. An initial polymer mass of about 15-20 mg is taken as 100% and this percentage decreases as the temperature increases, due to the mass loss corresponding to the water loss or decomposition of the polymers.

In this project, we have analysed the decomposition of several polymers (see **table 1**), which are potential candidates to be used as in the PAD process due to the presence of groups to bind the metal cations.

As we observe in **figure 10**, the decomposition temperatures of the polymers used are ranged between 500 and 640 °C. The polyacrylic acid (PAA) has the lowest decomposition, around 500 °C. In this polymer, there is a huge decrease up to 120 °C that it is related to the presence of water in the commercial PAA solution.

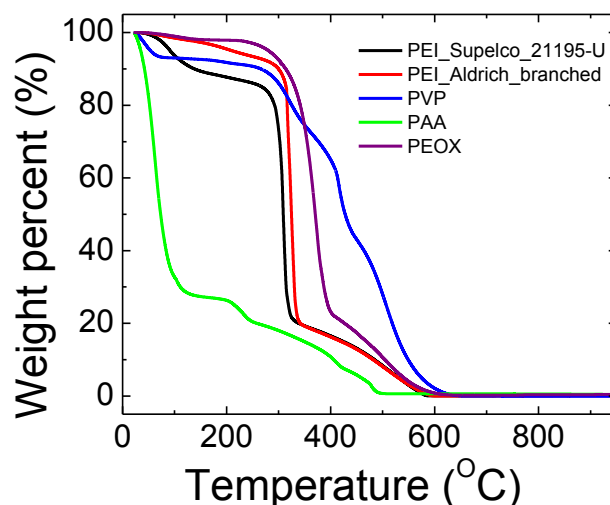


Figure 10. TGA curves to the different polymers used in depositions.

We can see that the two types of PEI have also a sharp drop in the curve because these are in solution; the loss of water is what causes these falls on the curve. Polyvinylpyrrolidone (PVP) and poly(2-ethyl-2-oxazoline) (PEOX) are in a solid state and therefore do not show so marked decrease in TGA curves.

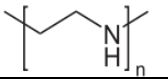
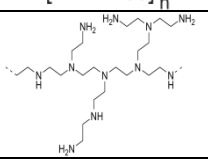
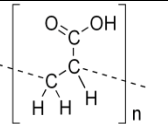
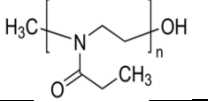
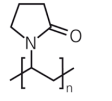
POLYMER	ACRONYM	FORMULA	DECOMPOSITION TEMPERATURE (°C)
<i>Polyethyleneimine -</i>	PEI		592
<i>Polyethyleneimine (branched)</i>	PEI (branched)		604
<i>Polyacrylic acid</i>	PAA		506
<i>Poly(2-ethyl-2-oxazoline)</i>	PEOX		637
<i>Polyvinylpyrrolidone</i>	PVP		657

Table 1. Decomposition temperatures values for polymers tested in this work.

5.2. Preparation and deposition of the solution.

We will describe the process of PAD using PEI as the polymer to form the solutions. Other polymers are still under evaluation but in order to close this project, we focused on the results obtained with PEI.

In the PAD process, the first step in the growth of our films is the preparation of solutions of the different used metals. For this purpose, we weigh a certain amount of hydrosoluble metal salt of the desired cations, and it is dissolved in a determined volume of water (25 mL) with ethylenediaminetetraacetic acid (EDTA, 1:1 molar ratio) and PEI (1:1 mass ratio to EDTA). The solutions are stirred to ensure uniform

distribution of complexes of metal cations. In the **table 2** shows the types of salts used by the preparation of the precursor solutions.

<i>Metal atom</i>	<i>Metallic salt</i>	<i>Reference</i>
<i>Sr</i>	<i>Sr(NO₃)₂ (>99.0%)</i>	<i>Fluka; CAS [10042-76-9]</i>
<i>Ru</i>	<i>RuCl₃·xH₂O (35-40% Ru)</i>	<i>ACROS ORGANICS; CAS [14898-67-0]</i>
<i>La</i>	<i>La(NO₃)₃·6H₂O p.a</i>	<i>Fluka; CAS [10277-43-7]</i>
<i>Mn</i>	<i>Mn(NO₃)₂·H₂O (>98.0%)</i>	<i>Alfa Aesar; CAS [17141-63-8]</i>
<i>Bi</i>	<i>Bi(NO₃)₃·xH₂O (99.999%)</i>	<i>Alfa Aesar; EINECS [233-791-8]</i>
<i>Fe</i>	<i>Fe(NO₃)₃·9H₂O (>98.0%)</i>	<i>SIGMA-ALDRICH; Cat.No. [21682-8]</i>

Table 2. *Metallic salt used to prepared the solutions.*

We used PEI from Supelco [*GC Stationary Phase, Supelco 21195-U*] or the branched version from [*SIGMA-ALDRICH CAS [9002-98-6]*, with average molecular weight~25.000 by LS and molar weight~10.000 by GPC]. EDTA was taken from *SIGMA-ALDRICH CAS [60-00-4; 607-429-00-8]*, with molecular weight: 292.24, assay >99% (titration), as complexing agent.

The following process is filtration of the solutions, an extremely important step because of the elimination of PEI molecules with a low molecular weight that can produce defects (surface deformation and fractures) in the films by decomposition in thermal treatment.

After taking a 100 µl aliquot of the solution and dilute 1:100, we carry out the determination of the cation concentration of cations using ICP analysis. Once known the concentration, we mixed and homogeneize the solutions of several cations in the stoichiometry ratio to obtain the precursor of solution according to the composition of the desired film. We take a necessary volume of this precursor solution with a micropipette, about 20-45 µl, and drop the volume on the substrate before starting the spin-coater. When we set the parameters, also for each case, we start the spin-coating process.

We have used SrTiO₃ (001) substrates because their cell parameter is close to that of the target films to be synthesized in this work. This means that the *f* parameter is small enough so that the strain between substrate and film is not too large.

Thermal treatment is the last step. The steps and final treatment temperature depend on the film to synthesize and the decomposition temperature of the used polymer. The thermal treatment sometimes requires a different atmosphere than the air, for this purpose a tube furnace is used with a mass flow controller in order to know exactly the used flow.

5.3. Synthesis of BiFeO₃ (BFO) thin films.

The concentration of the precursor solutions was 200,034mM and 119,878 mM for Fe and Bi cations respectively. We have mixed 0.72 ml of Bi-EDTA-PEI solution and 1.2 ml of Fe-EDTA-PEI (stoichiometry proportion) obtaining a final solution prepared for deposition with a total cationic concentration of ~150 mM. The mixture was spin-coated with the following deposition conditions:

- 20 µl final of solution.
- Rotation speed: 3000 rpm during 20 seconds.
- Substrate SrTiO₃ (001), with drying temperature of 120 °C.

Finally, after the deposition the films were annealing at 650°C during 3 hours (heating and cooling ramps of 2 °C /min) under two different atmospheres: in air and in nitrogen in order to study the effect of these different atmospheres in the synthesis of BFO. We have chosen a reducing nitrogen atmosphere taking into account the work of *H. Liu et al.* where the authors obtain pure BFO in bulk under H₂ and N₂ atmospheres.²⁹

Moreover, previous studies in the group showed no important differences in the decomposition temperature of PEI under N₂ with respect to air.

After the heat treatment, the next step is their structural characterization of the films using X-ray diffraction.

Figure 11 shows the XRD diffractogram for one of our samples. Only the (001) reflections appear for the STO substrate as well as the film, meaning that the film grows in the same orientation than the STO substrate. No secondary reflections of impurities

²⁹ H. Liu, Y. Pu, X. Shi, Q. Yuan, *Ceram. Int.* **39**, S217–S220 (2013).

or missorientations are observed. From this diffractogram we can obtain the value of the out of the plane lattice parameter for our samples.

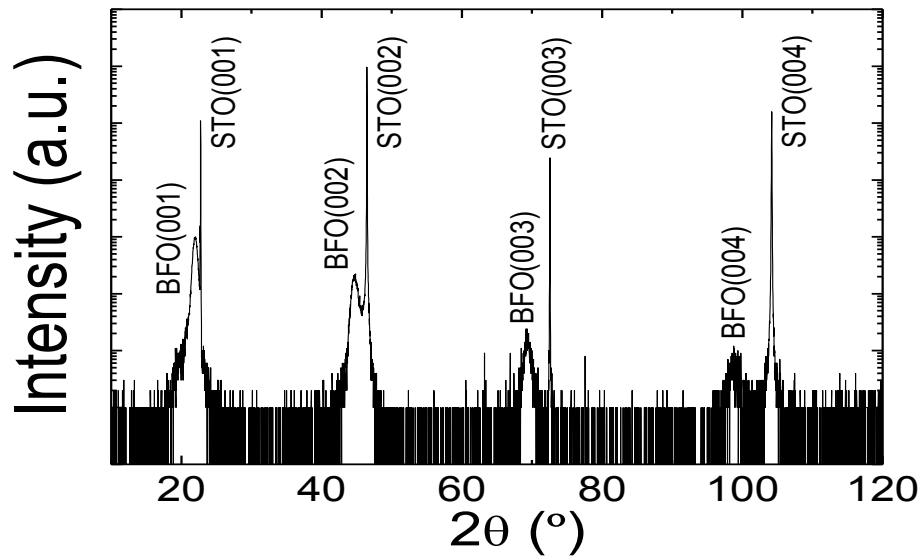


Figure 11. XRD diffractogram of BFO film treated in air at 650 °C.

To better display the graphical information provided by the XRD diffractogram, we do a more detailed measurement of the peak corresponding to the plane (002) because it is the most intense, and therefore tends to give us the same information but more clearer. It is true that sometimes peaks at higher angles such as the plane (004) give a greater separation between the signals of the substrate and the film, but in our particular case, we have taken the first option as a compromise of intensity and position with respect to the peak of the substrate.

In **figure 12**, X-ray diffractograms around the (002) reflection and XRR measurements are displayed for both samples (in air and nitrogen atmosphere).

We have also made reflectivity measurements of the films to obtain the values of the thickness, the interface roughness, and density of our materials (**figure 12 b and c**).

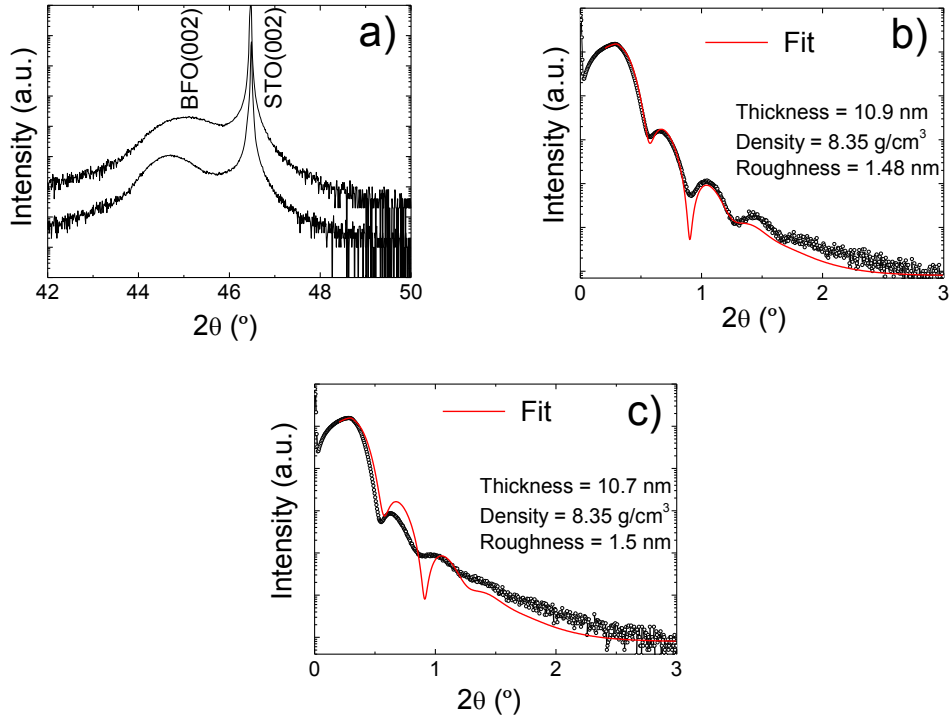


Figure 12. a) X-Ray diffractograms around the peak (002) for BFO @ STO in air (top) and N_2 (bottom) at 650 °C; b) XRR diffractogram for BFO grown in air atmosphere at 650 °C over STO (001); c) XRR diffractogram for BFO grown in N_2 at 650 °C on STO (001).

Through the fitting of the XRR measurements, we obtain the following parameters:

- The thickness of the films: in both atmospheres is around 11 nm.
- The roughness is about 1.5 nm.
- Material density is 8.35 g/cm^3 for both samples

From the XRD diffractogram we can obtain the out of the plane lattice parameter value using the formula described in the X-Ray Diffraction section (Experimental Part), the values are $4.029(1) \text{ \AA}$ and $4.051(1) \text{ \AA}$ for the sample grown in air and nitrogen atmosphere respectively. We see that the lattice parameter out of the plane for the film is greater than the BFO in bulk (3.964 \AA)^{19,20}, so the material undergoes an in-plane compressive stress. To confirm this, we have performed the reciprocal space maps (RSM) measurement (**figure 13**). We observe a good matching between the films and the substrate (in plane parameter = 3.905 \AA) and therefore conducting an in plane compressive stress.

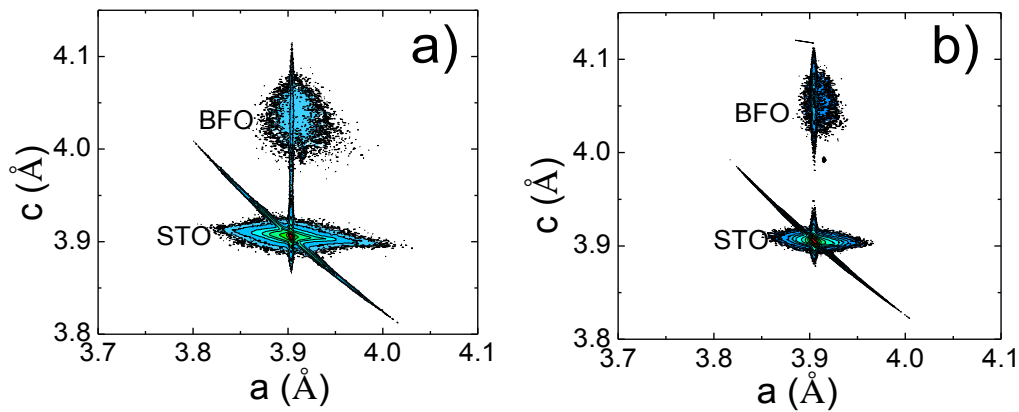


Figure 13. Reciprocal space maps of BFO samples grown at 650 °C in a) air atmosphere and b) N₂ atmosphere.

We can also see that the values obtained for the out of plane lattice parameters in **figure 13** present similar values to those obtained by XRD, 4.032 Å and 4,053 Å respectively for air and nitrogen atmosphere.

On the other hand, with these two parameters we can calculate the film volumes, and obtain information about whether the growth of our film involves an elastic deformation or present some kind of defect in the structure. The volume values are displayed in table X. We observe that there is a slight difference between the bulk and film volumes, that can mean small cation vacancies.

<i>Atmosphere</i>	<i>Cell volume in bulk (Å³)</i>	<i>Cell volume in film (Å³)</i>
<i>Air</i>	<i>62.29</i>	<i>61.45</i>
<i>N₂</i>	<i>62.29</i>	<i>61.77</i>

Table 3. Values for cell volume for the different BFO films synthesized at 650 °C.

After analysis of the data obtained from the diffractograms of XRD, XRR and RSM, a study of the surface of the BFO films was performed by AFM (atomic force microscopy). This study is useful to determine the surface roughness of our materials, and obtain the values of R_q (roughness mean square).

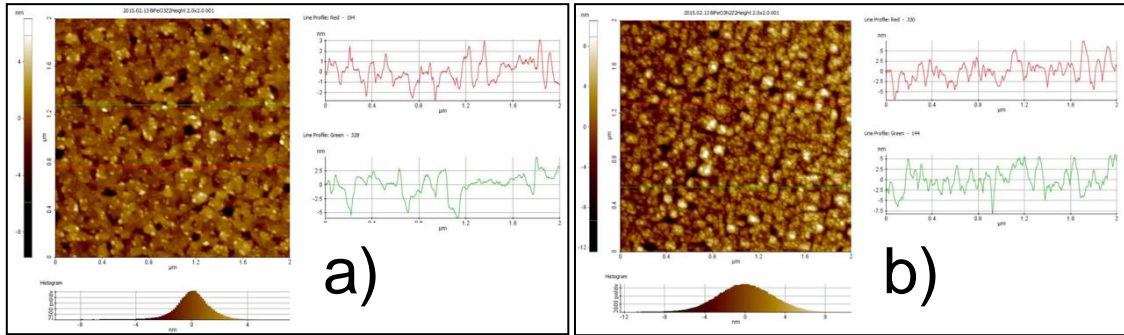


Figure 14. AFM images in no contact mode for BFO films in a) air atmosphere and b) N_2 atmosphere.

R_q values for both samples are 1.4 nm to BFO synthesized in air atmosphere and 2.6 nm to BFO synthesized in N_2 atmosphere. Moreover, the surface of the samples is not uniform due to segregation in our film are appreciated (white spots, **figure 14**). So we have carried out the synthesis of a new film at a lower temperature in order to try to avoid this segregation, considering the possibility of segregation of Bi and Fe oxides.

Taking also into account that the roughness is smaller (AFM) and the better defined oscillations in XRR of the samples synthesized in air, we decided to synthesized a new BFO film annealing at 600 °C in air.

The value obtained for parameters in the plane (a and b) is 3,905 Å and out of the plane parameter (c) is 4.03(1) Å, so we have a cell volume of 61.45 Å³.

This film is slight thicker than those synthesized at 650°C, around 15 nm, and its roughness is around 1.68 nm (**figure 15**).

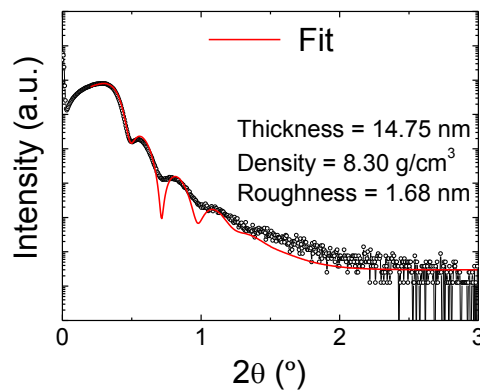


Figure 15. XRR diffractogram for the BFO sample grown at 600 °C in air atmosphere.

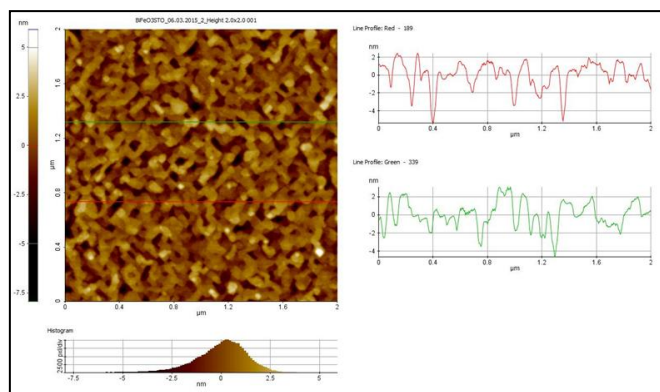


Figure 16. AFM image in no contact mode to BFO sample grown at 600 °C in air atmosphere.

The AFM image (**figure 16**) shows greater homogeneity in this sample than the samples synthesized at 650°C, and less segregation. So the choice of lower the temperature it has had a positive impact on the growth of film.

5.4. Synthesis of SrRuO₃ (SRO) thin films.

Prior to the SRO film growth we have carried out a study of stability of ruthenium (Ru) as our intention was to make a deposition using the same method of preparation of the solutions for the BFO.

We started with the preparation of solutions of ruthenium and EDTA concentrations in the range of 10^{-5} M, and via UV-Vis spectroscopy we performed a study of absorption bands corresponding to different Ru complexes. We studied the optimal pH for obtaining a complex with appropriate negative charges to establish the necessary interactions with the positive amino groups of the PEI and so achieve maximum retention of Ru cations.

As seen in **figure 17**, as the pH increases, the Ru-EDTA complex varies, obtaining a molecule with greater negative charge as the pH increases, as the complex lose H^+ . UV-Vis spectroscopy, **figure 17 b**, shows that around pH~ 7.4 the absorption band undergoes a change. The appearance of two bands in a different position than those for

lower pH indicates that the complex is undergoing a change in its structure that causes the change electronic transitions between states.

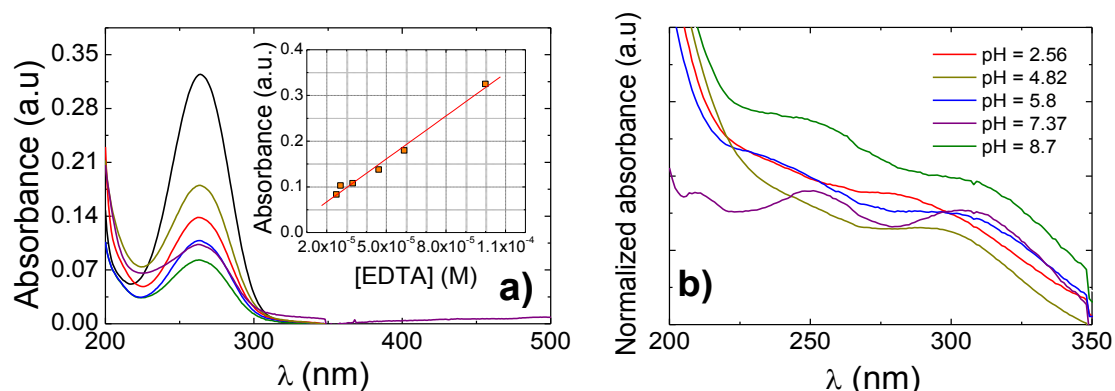


Figure 17. a) Representation of the absorption bands of EDTA in aqueous solution at different pH; b) Representation of the absorption bands Ru-EDTA complex in aqueous solution at different pH.

Also a study of aqueous solutions of EDTA was performed in the concentration range of 10^{-5} - 10^{-4} M to confirm that the spectrum of EDTA did not suffer evolution with pH variation (**figure 17 a**). The changes in the Ru-EDTA complex can be rationalized according to:³⁰

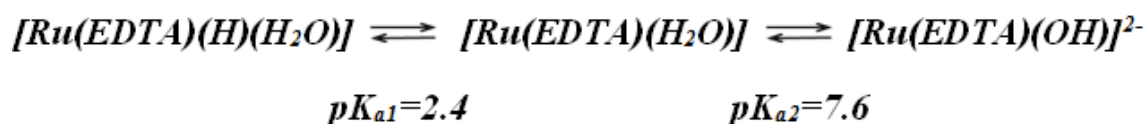


Figure 18. Complexes Ruthenium-EDTA equilibrium in water under pH changes.

The process carried out for the preparation of Ru-EDTA-PEI solution was the same as for the respective Bi and Fe, however, when attempting to stabilize the dissolution of Ru-EDTA-PEI, underwent hydrolysis of Ru and thus, the appearance of a precipitate mixture of oxide and hydroxide of Ru. The cause was the high pH at which forced us to work complexation with EDTA to obtain a negatively charged complex.

³⁰ H. C, Bajaj and R. van Eldik, *Inorg. Chem.* **27**, 4052-4055 (1988).

So, it was necessary to prepare a new solution to which the pH is exhaustively controlled by determining the hydrolysis-point around pH~5.5. The solution was filtered with MILLIPORE-equipment described above, with filter 10 kDa as solutions of other metals, and after sending an aliquot of the solution to ICP, the ruthenium concentration was 120.88 mM, it was not a very high value, but enough to try deposited this solution.

The pH of the solution after the filtration process was 5.21 and it wasn't appreciated the appearance of any precipitate. The final molarity of cations was 150.7 mM. Then Sr-Ru solution was concentrated to a value of 200.00 mM by solvent evaporation.

The conditions of deposition to conduct were:

- 20 μ l of solution.
- Rotation speed: 4500 rpm during 20 seconds.
- Substrate SrTiO₃ (001), with drying temperature of 140 °C.

The heat treatment was 700 °C in O₂ atmosphere and these conditions were maintained throughout successive depositions.³¹

However, the results obtained by the XRR and XRD diffractograms showed no signs of being we obtain the desired product. Furthermore, electrotransport tests showed us an insulating film, so that the product obtained was not SrRuO₃ (conductive). Therefore, since they have not been successful, we decided to carry out the synthesis using PAA as retention polymer, one polymer subject studied by TGA. We must be careful with the time of preparation of the solutions and the time between preparation and deposition of solutions for Ru-PAA and Sr-Ru-PAA, as they undergo gelification after a few minutes.

0.5 ml of Ru-PAA solution were taken and 0.3634 ml of Sr-PAA obtaining a concentration of cations, 269.51 mM in the deposition solution.

Although if heat treatment conditions are maintained (growing temperature and atmosphere), the deposition conditions change:

- 30 μ l of solution.
- Rotation speed: 2000 rpm during 20 seconds.³²

³¹ H. M. Luo, M. Jain, S. A. Baily, T. M. McCleskey, A. K. Burrell, E. Bauer, R. F. DePaula, P. C. Dowden, L. Civale, and Q. X. Jia, *J. Phys. Chem. B* **111**, 7497-7500 (2007).

- Substrates SrTiO₃ (001) and LaAlO₃ (001), with drying temperature of 140 °C.

In this case the heating ramp in O₂ atmosphere has 3 steps:

- 2 °C/min from 25 °C to 150 °C in this step is maintained 10 min.
- 3 °C/min from 150 °C to 460 °C keeping it at that temperature for 30 min.
- 3 °C/min from 460 °C to 700 °C, the final growth temperature, and this temperature is maintained for 1 hour.

The cooling ramp is 5 °C per minute to room temperature.

In **figure 19** we can see the results of X-ray diffraction patterns of the peak detailed film (002) grown on two different substrates.

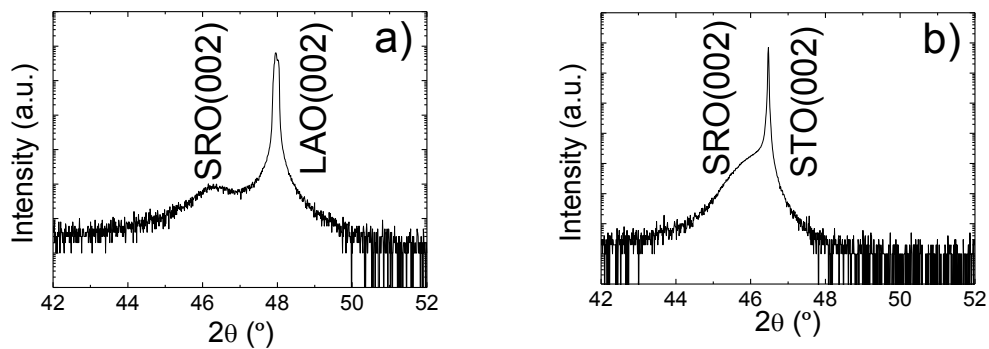


Figure 19. a) Detailed XRD diffractogram to SRO of peak (002) grown on LaAlO₃ (LAO)(001) at 700 °C and under an O₂ atmosphere; b) Detailed XRD diffractogram to SRO of peak (002) grown on STO (001) at 700 °C and under an O₂ atmosphere.

We tried a deposition on LaAlO₃, LAO ($a_{pc} = 3.79 \text{ \AA}$)³² to probe the effect of a larger compression over the easiness of synthesis of the film.

We obtained lattice parameter values outside the plane of 3.918(2) Å for the film grown over LAO and 3.945(1) Å for the film grown over STO, knowing that the lattice parameter value of SRO in bulk is 3.93 Å.²² These values indicate that the film grows with a compression tension out of the plane to STO but relaxed on LAO. In the RSM for the sample over STO, it can be seen that the sample adjusts its lattice parameter to the substrate (**figure 20**).

³² S. Y. Park and Y. P. Lee, *J. Korean Phys. Soc.* **45**, 47-45 (2004).

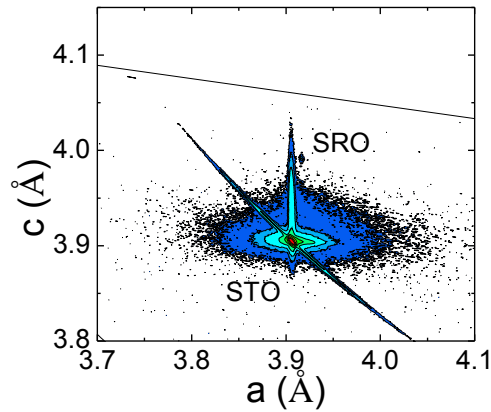


Figure 20. RSM diffractogram of SRO film synthesized on STO (001) by the method of PAD using polyacrylic acid as a polymer.

Resistance measurements of the samples were also carried out to check the electrical transitions of the film, and therefore its quality. The SRO has a metallic behavior with a transition around 140 K as can be seen in **figure 21**. The SRO has a Curie temperature about 160 K in bulk.²¹ Data obtained from the electrical transport study indicate a slight reduction in the position of the electrical transition temperature due to the strain on the film to adjust its lattice parameters on the plane to the STO. However, the electrical measurement on LAO sample shows that this film is insulator, meaning that the product obtained was not stoichiometric SrRuO₃.

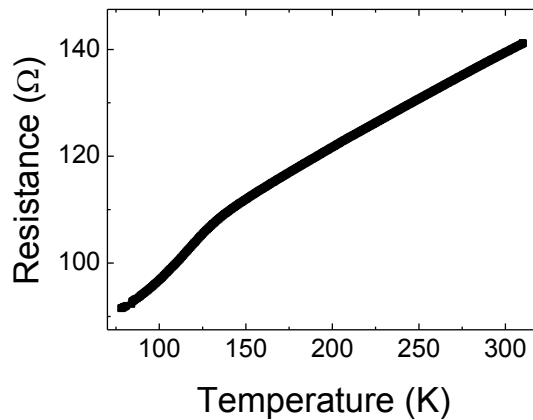


Figure 21. Graphical representation of the electrical behavior of a film of SRO synthesized by the method of PAD as a function of temperature.

In any case, these results confirm the possibility of fabricating epitaxial thin films of SRO on STO by this chemical method, keeping the electrical properties characteristic of this important material.

5.5. Synthesis of $\text{La}_{0.7}\text{Sr}_{0.3}\text{MnO}_3$ (LSMO) thin films.

For the preparation of LSMO-EDTA-PEI solution, precursor solutions have been used with the complexing agent and polymer dissolved with the respective metal hydrated nitrates that are part of the film structure. The cation concentration and volume taken from each solution are listed in **table 4**.

<i>Metal solution</i>	<i>Metal concentration (mM)</i>	<i>Volume taken (mL)</i>
<i>La-EDTA-PEI</i>	<i>96.106</i>	<i>5.993</i>
<i>Sr-EDTA-PEI</i>	<i>51.016</i>	<i>4.839</i>
<i>Mn-EDTA-PEI</i>	<i>175.06</i>	<i>4.7</i>

Table 4. Concentration and volume taken from precursor solutions to prepare the final deposition solution.

The final concentration of our solution was 105.95 mM. The solution was concentrated to 2 ml obtained final cationic concentration of 150 mM. The deposition conditions were:

- 35 μl of solution.
- Rotation speed: 4500 rpm during 20 seconds.
- Substrate SrTiO_3 (001), with drying temperature of 120 $^{\circ}\text{C}$.

Thermal treatment was conducted in a muffle furnace at 950 $^{\circ}\text{C}$ with heating and cooling ramps of 1 $^{\circ}\text{C}/\text{min}$, in air atmosphere.

The processing of data provided by XRD diffractogram (**figure 22 a**) show that LSMO reduced its lattice parameter out of the plane (compressive stress), which is a good signal that has been adjusted to STO substrate ($a_c=3.905 \text{ \AA}$) and therefore undergoes an elongation in their parameters in the plane. This is confirmed by the RSM diffractogram

which shows an adjustment to the STO substrate in the lattice parameter in the plane (**figure 22 b**). We obtained a value of the lattice parameter out of the plane 3.866 \AA , (in bulk = 3.88 \AA).²⁴

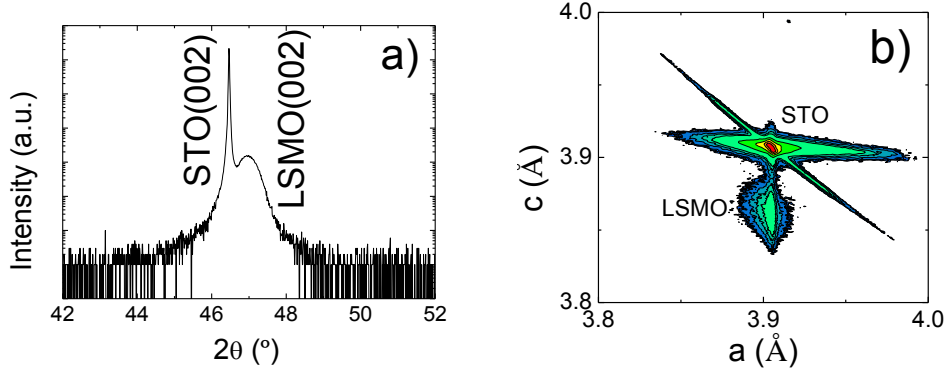
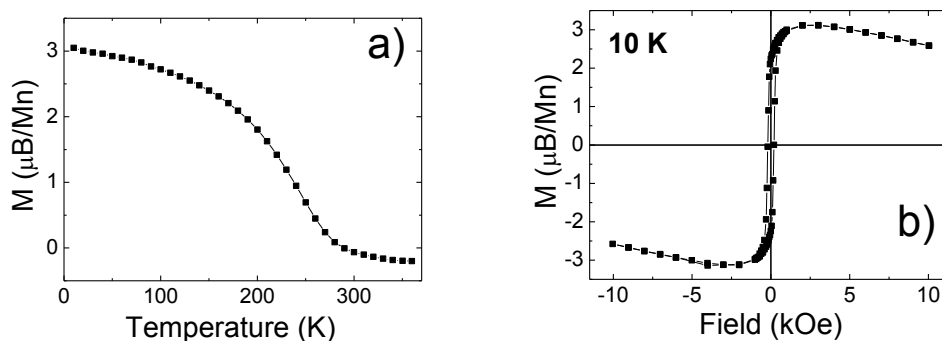


Figure 22. a) Detailed XRD diffractogram to LSMO of peak (002) grown on STO oriented along (001); b) RSM diffractogram to LSMO grown on STO oriented along (001).

Data from resistance versus temperature graphic indicates a semiconductor behavior with a clear transition around 285 K (**figure 23 c**). We have also made magnetic measurements for our sample of LSMO (**figure 23 a**) and we have verified that the ferromagnetic to paramagnetic Curie temperature is around 285 K. The low temperature coercivity and saturation magnetization, shown in the $M(H)$ curve at 10 K are around 0.2 kOe and $3 \mu_B/\text{Mn}$, respectively (**figure 23 b**). These values deviate slightly from the values in the bulk.



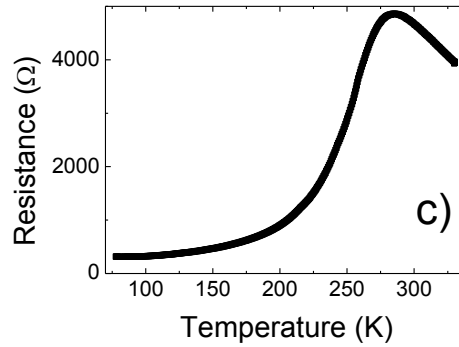


Figure 23. Graphical representation to LSMO thin film synthesized by PAD method: a) magnetic response vs temperature; b) hysteresis curve; c) resistance vs temperature.

The value to the Curie temperature to LSMO in bulk is around 340 K, the change in transition position (Curie temperature) is indicating an alteration of the sample stoichiometry, caused by errors in the preparation of the solutions, ICP measurements or segregation of strontium oxides during thermal treatment. The value of T_C for thin films falls between 2.8 and 8.9 nm³³, but in our case, X-rays indicate a thickness of 15 nm, so that the appearance of vacancies in the material Sr is highly likely.

Therefore, although the films were formed, their properties differ slightly from bulk, and so the conditions for LSMO deposition must be further optimized.

5.6. Synthesis of a bilayer: BiFeO₃ on La_{0.7}Sr_{0.3}MnO₃ on SrTiO₃ substrate (BFO/LSMO@STO).

The growth process of the bilayer was performed by two consecutive depositions on the same substrate of STO (001) using the same deposition solutions in the study of each film grown previously, and under the same conditions of deposition. First we deposited LSMO on STO (001) substrates, after the thermal treatment, the LSMO film is synthesized and then we deposit another layer, this time of BFO. So the higher layer is BFO and the lower layer is the substrate with an intermediately BFO layer.

³³ F. Sandiumenge, J. Santiso, L. Balcells, Z. Konstantinovic, J. Roqueta, A. Pomar, J. P. Espinos and B. Martínez, *Phys. Rev. Lett.* **110**, 107206 (2013).

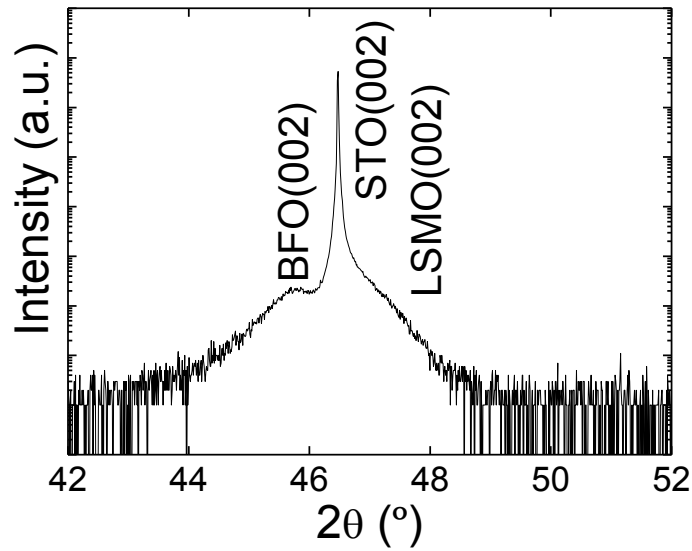


Figure 24. The XRD diffraction pattern for a bilayer of BFO/LSMO synthesized by PAD method.

XRD diffractogram for the bilayer (**figure 24**) shows the values of cell parameters out of the plane for both layers, the BFO is 3.953(1) Å, greater than the value in bulk (compression in lattice parameters in the plane) and the value of LSMO is 3.872(4) Å, less than the value in the massive material (elongation in lattice parameters in the plane).

But to ensure that both the lower layer and the upper fit the lattice parameter of the substrate, we performed detailed RSM analysis where we check if the lattice parameters in the plane for both layers correspond to the substrate. This was indeed the result as observed in **figure 25**.

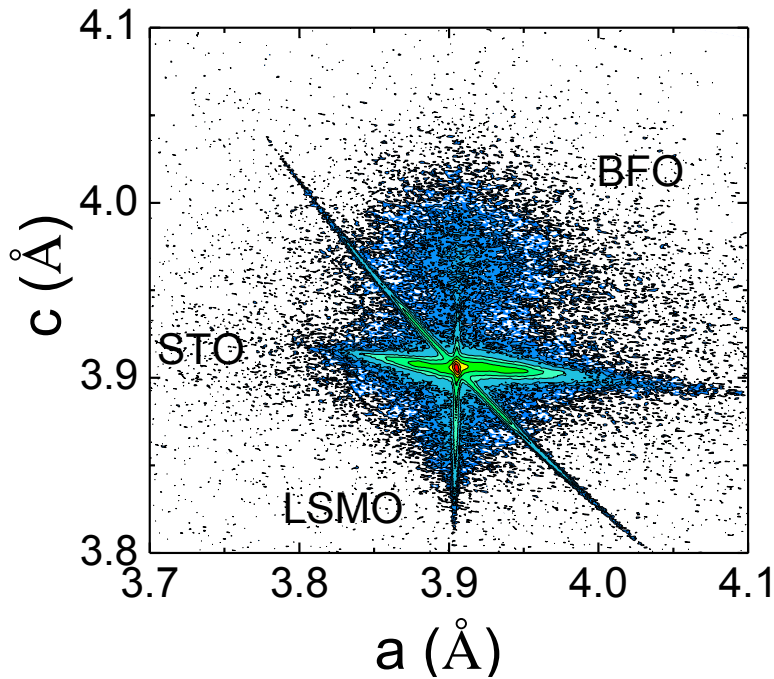


Figure 25. RSM diffractogram obtaining to the bilayer of BFO/LSMO synthesized by PAD method.

Both films are set correctly to lattice parameter in the plane of the substrate, giving lattice parameter values out of the plane (3.962\AA to BFO and 3.876) that confirm those obtained in the XRD diffractogram (**figure 24**); obtaining a cell volumes of 60.28\AA^3 to BFO (62.29\AA^3 in bulk) and 59.04\AA^3 to LSMO (58.46\AA^3 in bulk). We notice a slight volume decrease in the BFO layer compared to that obtained in the thinner isolated layer (volume around 61.5\AA^3). This feature can be produced by cation vacancies owing to a worse growth of the BFO layer on the LSMO layer.

Therefore, we can see that the induced strain by adjusting lattice parameters in the plane to substrate not only affect the first layer (LSMO) but also to the second layer (BFO).

6. CONCLUSIONS.

Polymer Assisted Deposition (PAD) is a competitive method to obtain high quality thin films with nanometric thickness.

We have managed stoichiometric solutions to depositions, stable over time.

In this project we achieved growth of three materials with different nature and properties:

- Obtaining BiFeO_3 over SrTiO_3 monocrystalline substrates with an epitaxial growth.
- Obtaining SrRuO_3 over SrTiO_3 monocrystalline substrates with an epitaxial growth.
- Obtaining $\text{La}_{0.7}\text{Sr}_{0.3}\text{MnO}_3$ over SrTiO_3 monocrystalline substrates with an epitaxial growth. In this case the process must be further optimized in order to obtain stoichiometric samples.
- Obtaining a bilayer $\text{BiFeO}_3/\text{La}_{0.7}\text{Sr}_{0.3}\text{MnO}_3$ over SrTiO_3 monocrystalline substrates with epitaxial growth in both materials.